NbCycB2 represses Nbwo activity via a negative feedback loop in the tobacco trichome developmemt

Minliang Wu[1, 3], Yuchao Cui[1], Li Ge[1], Lipeng Cui[1], Zhichao Xu[1], Hongying Zhang[2], Zhaojun Wang[2], Dan Zhou[1], Shuang Wu[3], Liang Chen[1,*], Hong Cui[2,*]

1. Xiamen Key Laboratory for Plant Genetics, School of Life Sciences, Xiamen University, Xiamen 361102, China

2. Key Laboratory for Cultivation of Tobacco Industry, College of Tobacco Science, Henan Agricultural University, Zhengzhou, 450002, China

3. FAFU-UCR Joint Center and Fujian Provincial Key Laboratory of Haixia Applied Plant Systems Biology, College of Horticulture, Fujian Agriculture and Forestry University, Fuzhou 350002, China

* Co-Corresponding author (email: chenlg@xmu.edu.cn, cuihonger_13@163.com)

Running title: Reciprocal regulation between *Nbwo* and *NbCycB2*

Highlight

NbCycB2 is specifically expressed in trichomes of *Nicotiana benthamiana* and represses the Nbwo activity via a negative feedback loop in tobacco trichome developmemt.

Abstract:

The wo protein and its downstream gene, *SlCycB2* have been demonstrated to regulate the trichome development in tomato. It was shown that only gain-of-function mutant form of *wo*, Wo^V (*wo* woolly motif mutant allele) could induce the increase of trichome density. However, it is still unclear the relationships between wo, Wo^V and *SlCycB2* in trichome regulation. In this study, we demonstrated Nbwo ($NbWo^V$) directly regulated the expressions *NbCycB2* by binding to the promoter of *NbCycB2* and its genomic sequences. As a feedback regulation, NbCycB2 negatively regulates the trichome formation by repressing Nbwo activity at protein level. We further found that the mutations of Nbwo woolly motif could prevent repression of $NbWo^V$ by NbCycB2, which results in the significant increase of active *Nbwo* proteins, trichome density and branches. Our results revealed a novel reciprocal mechanism between *NbCycB2* and *Nbwo* during the trichome formation in *Nicotiana benthamiana*.

Key word: Feedback loop; Trichome formation; Nbwo; NbCycB2; Woolly motif; L1-like box

Introduction

Trichomes are the specialized epidermal protuberances locating on aerial parts of nearly all terrestrial plants. They can be classified into various types by cell numbers

61 and shapes -- unicellular/multicellular, and glandular/non-glandular. In *Arabidopsis*, it
62 has been well-elucidated that the development of trichomes (unicellular and
63 non-glandular), is regulated by the trimeric MYB-bHLH-WDR protein activators
64 complex (GL1 (Oppenheimer et al., 1991)-GL3/EGL3 (Payne et al., 2000)-TTG1(Walker
65 et al., 1999)). This transcriptional complex activates the expression of the
66 homeodomain protein GLABROUS2 (GL2) to induce the formation of trichomes
67 (Rerie et al., 1994; Grebe, 2012). In addition, it triggers the expression of the single
68 repeat R3 MYBs (including TRY (Schnittger et al., 1999), CPC (Wada et al., 1997), ETC1,
69 ETC2, ETC3 (Kirik et al., 2004; Wester et al., 2009) and TCL2 (Gan et al., 2011)) which
70 act as negative regulators of GL3 or EGL3 by forming a repressor complex
71 (GL3/EGL3-TRY/CPC-TTG1) in trichome development (Wang et al., 2008; Wester et al.,
72 2009). Thus the control of trichome development in *Arabidopsis* requires a
73 regulatory loop including both activators and repressors (Grebe, 2012; Pattanaik et
74 al., 2014).
75 The trichomes are multicellular glandular (GSTs) structure in approximately 30% of
76 all vascular plants (Glas et al., 2012). Since many phytochemicals and compounds
77 with economical values can be synthesized and secreted by multicellular GSTs
78 (Mauricio and Rausher, 1997; Hollósy, 2002; Valkama et al., 2003; Freeman and
79 Beattie, 2008), multicellular glandular trichomes have considerable economic
80 pontential (Sallets et al., 2014; Huchelmann et al., 2017). However, it has been
81 demonstrated that the networks regulating unicellular trichomes did not work in the
82 development of multicellular trichomes (Serna and Martin, 2006; Yang et al., 2011;
83 Kang et al., 2016; Yan et al., 2016).
84 In tomato, a HD-ZIP IV transcriptional factor, wo protein has been demonstrated to
85 regulate the trichome initiation (Yang et al., 2011). This HD-ZIP IV member contains
86 four conserved domains including homeodomain domain (HD), the leucine zipper
87 domain (LZ), the steroidogenic acute regulatory protein-related lipid transfer (START)
88 and the START-adjacent domain (SAD). However, overexpression of *wo* failed to
89 induce the change of trichome density, and only ectopic expression of its
90 gain-of-function mutant alleles, Wo^{V}, could cause higher density of trichomes in

91 tomato (*Solanum lycopersicum*) and tobacco (*Nicotiana tabacum*) (Yang et al., 2011;
92 Yang et al., 2015). The *Wo*^{V} allele has two point mutations at the C-terminal domain
93 (Since this motif was conserved in the most wo alleles, we name it as woolly motif in
94 this study). The sequence analysis revealed that wo protein is more similar to
95 PROTODERMAL FACTOR2 (PDF2) and the PDF2 redundant protein -- ARABIDOPSIS
96 THALIANA MERISTEM L1 (ATML1), both of which are involved in shoot epidermal cell
97 differentiation (Abe et al., 2001; Ogawa et al., 2015), than GL2 in *Arabidopsis*.
98 In *Arabidopsis*, the ectopic expression of a constitutive active B-type cyclin induced
99 mitotic divisions and resulted in the increase of multicellular trichomes (Schnittger et
100 al., 2005). *SlCycB2*, a hypothetical B-type cyclin, was reported to directly interact with
101 wo to promote the development of type I trichome (Yang et al., 2011; Yang et al.,
102 2015). Its homologous protein in *Arabidopsis* (AT5G06270) was also found to interact
103 with GL2 or co-repressor TOPLESS proteins (Wu and Citovsky, 2017b, a). However, as
104 reported in a recent study, overexpression of *SlCycB2* resulted in non-trichome
105 phenotype, while suppression of *SlCycB2* promoted trichomes formation in tomato
106 (Gao et al., 2017). These inconsistent results raise the important questions: what is
107 the function of *SlCycB2* in trichome formation and why the mutation of woolly motif
108 can promote trichome formation?
109 Similar to tomato, trichomes in *Nicotiana benthamiana* are typically multicellular
110 structures, and almost all of the trichomes in *N. benthamiana* are glandular (Fig. S1),
111 making it a better system for studying glandular trichomes than tomato. In addition,
112 the genome map of *N. benthamiana* has been constructed (Bombarely et al., 2012).
113 Thus tobacco represents an excellent model plant to study the molecular mechanism
114 of multicellular trichome formation (Goodin et al., 2008). In this study, we cloned the
115 homologues of *wo* and *SlCycB2* in *N. benthamiana* (named *Nbwo* and *NbCycB2*), and
116 constructed a two-point mutantion *Nbwo* allele, *NbWo*^{V}. To investigate their
117 biological functions in trichome development, we constructed overexpression and
118 suppression transgenic lines of all genes. We demonstrated that Nbwo could
119 positively regulate the expression of *NbCycB2* through targeting to the cis-element in
120 *NbCycB2* promoter and its genomic DNA sequence. On the other hand, NbCycB2

121 could be a negative regulator of multicellular trichomes by directly binding and
122 inhibiting Nbwo activity. The previous identified mutation in woolly motif ($NbWo^V$)
123 blocked the interaction between NbCycB2 and Nbwo, removing the repression of
124 *Nbwo* by NbCycB2 and resulting in increased trichome density. Our results revealed
125 the mechanisms of the interaction between *Nbwo* and *NbCycB2* in regulating the
126 development of glandular trichomes.
127

128 **Materials and Methods**

129 **Plant materials and growth conditions**

130 Sterilized seeds of *N. benthamiana* were germinated and grown to seedlings on
131 MS medium, which solidified with 0.8% (w/v) gellan gum under 26 °C, 14 h light/10 h
132 dark conditions. Two-week-old plants were transferred to other sterilized bottle (for
133 genetic transformation) or soil in pots to grow to maturity. All wild type and
134 transgenic plants were grown in greenhouse under 26 °C, 14 h light/10 h dark
135 condition.

136 **Sequence analysis**

137 The protein sequences of the homologues of *wo* and *SlCycB2* were downloaded
138 from NCBI database (http://www.ncbi.nlm.nih.gov/) and Sol genomic network
139 (Fernandez-Pozo et al., 2015) (https://solgenomics.net/). In order to further analyze
140 the grouping and relatedness, the aligned sequences were used to construct the
141 phylogenetic trees in MEGA 5 by using the maximum-likelihood (ML) criterion with
142 100 bootstrap analysis. In addition, the relative conservation for each amino acid
143 position in the protein sequences of Nbwo and NbCycB2 was evaluated via WebLogo
144 (https://weblogo.berkeley.edu/) (Crooks et al., 2004), followed by the prediction of
145 their conserved domains in SMART program (https://smart.embl-heidelberg.de/)
146 (Letunic and Bork, 2018).

147 **RNA extraction and Real-time PCR**

148 Total of RNA was extracted from various tissue of plants by using the Eastep®Super
149 Total RNA Extraction Kit (Promega). The cDNA was synthesized from Dnase I treated
150 total RNA using M-MLV 1st Strand Kit (Invitrogen). Real-time PCR (qRT-PCR) was

151 determined by using SYBR Premix Ex Taq II (TaKaRa) and performed on ABI Stepone
152 real-time PCR system (Applied Biosystems). L25 ribosomal protein (L18908) was used
153 as an endogenous control (Schmidt and Delaney, 2010). Relative expression levels
154 were determined as described previously (Guo et al., 2016). Primers are listed in
155 Table S1.

156 **Plasmid construction and *N. benthamiana* transformation**

157 To investigate the biological functions of *wo* and *SlCycB2* in *N. benthamiana*, the
158 full-length coding sequences of two alleles of *Nbwo* and *NbCycB2* were amplified
159 with NheI and BamHI, XbaI and BglII cloning sites respectively from the general cDNA
160 of leaves (All the primers used in current study are provided in Table S1). In addition,
161 to confirm the function of the tomato Wo^V gene in tobacoo trichome formation (Yang
162 et al., 2015), an allele $NbWo^V$ with two point mutations at the locus 2084 (T was
163 replaced with G, result in Ile-697 changed to Arg) and 2092 (G was replaced with T,
164 result in Asp-700 changed to Tyr, Fig. S2c) of *Nbwo* was generated in *N. benthamiana*
165 by using a Mutagenesis Kit (Toyobo).

166 To construct the overexpression (OE) lines of *Nbwo*, $NbWo^V$ and *NbCycB2*, these
167 fragments were inserted into pCXSN-HA (Nbwo and $NbWo^V$ fused with HA tag) and
168 pCXSN-FLAG (NbCycB2 fused with Flag tag) vectors respectively under the control of
169 CaMV 35S promoter (Chen et al., 2009). The suppression expression constructs of
170 *Nbwo* and *NbCycB2* were performed by recombining with the RNAi vector
171 pH7GWIWGII with LR Clonase II enzyme (Invitrogen).

172 To comprehensively understand the expression sites of *NbCycB2*, approximate
173 2880bp upstream promoter fragments were amplified by PCR using the primers
174 shown in Table S1. The promoter fragments were then inserted into the
175 corresponding site of pH2GW7 vector to create the promoter-driven GFP-GUS
176 transformation by using Pro-*NbCycB2*: GFP-GUS gene fusion (Cui et al., 2015).

177 All of these constructs were transferred into *Agrobacterium tumefaciens* strain
178 GV3101, which were used to generate transgenic lines by using
179 *Agrobacterium*-mediated transformation. The gene expression levels in the
180 transgenic lines were examined by real-time PCR and western blot.

181 **Subcellular localization and tissue distribution**

182 The pCXDG vector (Chen et al., 2009) was used to analyse the subcellular
183 localization of *Nbwo*, *NbWo*^{V} and *NbCycB2*, which were fused with GFP driven by the
184 CaMV 35S promoter (p35s:GFP-*Nbwo*, p35s:GFP-*NbWo*^{V}, p35s:GFP-*NbCycB2*).
185 Transformants carrying these constructs were obtained as described above and then
186 transiently transformed into 4-week-old *N. benthamiana* leaves. After cultivation in
187 lowlight conditions for 48-72 h, GFP was observed using confocal microscopy (LSM
188 780, Carl Zeiss, Jena, Germany) with staining in DAPI solution (1 mg/ml) for 15 min
189 before observation.

190 The tissue distribution assays were performed as described in the previous study
191 (Jefferson et al., 1987). GUS staining was repeated at least three independent
192 transgenic lines.

193 **Yeast hybrid assays**

194 Yeast one-hybrid assays were performed to test the specific function area of
195 *NbCycB2* promoter binding Nbwo. The promoter of *NbCycB2*, separated into 5
196 fragments (E: -1027 ~ -831 bp, D: -830 ~ -631 bp, C: - 630 ~ -411 bp, B: -410 ~ -201 bp,
197 A: -200 ~ -1bp, Fig. 2a), were amplified and inserted into the pHIS 2 vector (Clontech)
198 (*NbCycB2*proE, *NbCycB2*proD, *NbCycB2*proC, *NbCycB2*proB, *NbCycB2*proA). Further
199 investigation of the targeted sequences in *NbCycB2* promoter were conducted by
200 point mutations in the two L1-like boxes in the D fragment (*NbCycB2*proD-m1,
201 mutant one L1-like box, changed 5'-GCAAATATTTACTC-3' to 5'-GCGGGTGACTC-3';
202 *NbCycB2*proD-m2, mutant two L1-like boxes, changed 5'-GCAAATATTTACTC-3' to
203 5'-GCGGGTGACTC-3', and 5'-ATTTACTC-3' to 5'-GGGACTCC-3'). To test the specific
204 region of *Nbwo* genomic sequence binding itself, four genomic fragments of *Nbwo*
205 (G1, -8 ~ 251 bp, include T3 fragment; G2, 2169 ~ 2522 bp, include T4 fragment; G3,
206 3485 ~ 3780 bp, include T5 fragment; G4, 4333 ~ 4660 bp, include T6 fragment, Fig.
207 7a), were amplified and inserted into the pHIS 2 vector (Clontech) (*Nbwo-G1*,
208 *Nbwo-G2*, *Nbwo-G3*, *Nbwo-G4*). In addition, the CDSs of *Nbwo* and *NbWo*^{V} were
209 inserted into vectors pGADT7 containing the GAL4 activation domain (AD) (Clontech).
210 The plasmids were co-transformed into the Y187 yeast strain, empty AD vector was

211 provided as the negative control, and cultivated on SD/-Leu/-Trp (-L-W) medium and
212 tested on SD/-Leu/-His/-Trp (-L-W-H) with 60 mM 3-amino-1,2,4-triazole (Sangon
213 Biotech (Shanghai) Co., Ltd) medium.

214 The yeast two-hybrid was performed to understand the interaction between *Nbwo*
215 and *NbCycB2*. We truncated *Nbwo* into four segments containing: HD, LZ, START and
216 SAD domains, and fused them into AD vectors to find the target region of the
217 interaction in *Nbwo*. In addition, the CDS of *NbWo*^{V} was also amplified and inserted
218 into AD vector. Each pair of AD and BD plasmids were co-transformed into the
219 Y2HGold yeast strain. BD-53 and AD-T constructs were co-transformed in to Y2HGold
220 as positive control, and BD-Lam and AD-T as negative control. The transformants
221 were then cultivated on SD/-Leu/-Trp medium (DDO) and tested on SD/-Ade/
222 -Leu/-His/-Trp with 40 mg/L X-a-Gal (QDO/X) or SD/-Ade/-Leu/-His/-Trp with 40 mg/L
223 X-a-Gal and 400 μg/L Aureobasidin A medium (QDO/X/A).

224 Yeast three-hybrid was conducted to analyze the binding competition between
225 Nbwo LZ domain (Nbwo-LZ) and NbCycB2 to Nbwo. The Nbwo-LZ was fused with BD
226 (Clontech). The *NbCycB2* was inserted into the downstream of methionine
227 repressible promoter (PMet25: *NbCycB2*) in pBridge vector. The plasmid of
228 BD-*Nbwo-LZ* was transferred with AD-*Nbwo* as positive control, and empty pBridge
229 vector was transferred to with AD-*Nbwo* as negative control. The transformants
230 were then tested on SD/-Ade/-Leu/-His/-Trp mediums with different concentrations
231 of methionine (0, 250 μM).

232 **Bimolecular fluorescence complementation Assay (BiFc)**

233 In order to determine the interaction of NbCycB2 and Nbwo (or NbWo^{V}) in *N.*
234 *benthamiana* protoplasts. The CDSs of *Nbwo*, *NbWo*^{V} and *NbCycB2* were inserted
235 into the pSAT6-cEYFP-C1-B vector (2x35s: YFP^{c}-*Nbwo*, 2x35s: YFP^{c}-*NbWo*^{V}) and the
236 pSAT6-n(1-174)EYFP-C1 vector (2x35s: YFP^{n}-*NbCycB2*) separately (Citovsky et al.,
237 2006). Each pair of the two plasmids were then transiently transformed into the
238 protoplasts via PEG–calcium transfection method as described in the previous study
239 (Yoo et al., 2007).

240 Moreover, to determine the interactions between Nbwo and NbCycB2 in vivo, the

241 CDSs of *Nbwo*, *NbWo*^{V} and *NbCycB2* were fused separately with the C-terminal
242 fragment of YFP in p2YC vector; *Nbwo*-LZ and *NbWo*^{V} were also fused with the
243 N-terminal fragment of YFP in p2YN vector respectively (Shen et al., 2011). Different
244 plasmid combinations were co-infiltrated into leaves of *N. benthamiana* as described
245 in previous study (Shen et al., 2011).

246 The YFP fluorescence was observed by using confocal microscopy (LSM 780, Carl
247 Zeiss, Jena, Germany). Before the observation, the transformed protoplasts were
248 cultivation in 26 °C for 12 h, and the transformed leaves of *N. benthamiana* were
249 cultivation in darkness for 48-72 h. Three biological repeats were observed
250 independently for each samples.

251 **Dual-luciferase (Dual-Luc) assay**

252 The regulatory effectors of 2x35s: *HA-Nbwo*, 2x35s: *HA-NbWo*^{V} and 2x35s:
253 *Flag-NbCycB2* were generated by using the DNA sequences with NcoI (5'-end) and
254 BglII (3'-end) cloning sites.

255 The firefly luciferase reporters were created by inserting the B and D fragments of
256 the *NbCycB2* promoter, and the *Renilla* luciferase was driven by the 35S promoter in
257 the pGreen-0800-II report vector (35S: REN-*NbCycB2*proB: LUC, 35S:
258 REN-*NbCycB2*proD: LUC). The mutants of the *NbCycB2* promoter D fragments were
259 also constructed using a Mutagenesis Kit (35S: REN-*NbCycB2*proD-m2: LUC). The
260 regulatory effector and the reporter were used at the ratio of 5:1 or 5:5:1 for the
261 expression test of two or three plasmids.

262 **Immunoblotting, CO-IP and pull-down assay**

263 The *N. benthamiana* leaves (~0.5 g) were homogenized with liquid nitrogen and
264 then solubilized with 0.4 ml of lysis buffer (25 mM Tris-HCl, 2.5 mM EDTA, pH 8.0,
265 0.05% v/v NP-40, 5% glycerol, 150 mM NaCl, 1 mM phenylmethylsulfonyl fluoride
266 and 20 uM MG132) for 30 min at 4 °C. After solubilization, the protein extract was
267 centrifuged at 13,000g for 10 min at 4 °C to separate the solubilized (supernatant)
268 and non-solubilized material. Total protein (~80 μg) was then used for the
269 immunoblotting assay. After SDS–PAGE separation, the proteins were
270 electrophoretically transferred to a PVDF membrane for immunodetection.

271 The interaction of NbCycB2 and Nbwo dimers were determined by using co-IP
272 assay in *N. benthamiana* protoplasts. In the expression vectors, the Nbwo protein
273 was fused to the HA and Flag tags, respectively, and the NbCycB2 was fused to the
274 GFP tag. Each pairs of the plasmids were transformed into the protoplasts via
275 PEG–calcium transfection method as described in the previous study (Yoo et al.,
276 2007). The total proteins were extracted by using lysis buffer and then incubated for
277 3 h at 4°C with 20 ul of Anti-HA Affinity Gel (Millipore). The immunoprecipitates were
278 washed five times with lysis buffer. The isolated proteins were detected by
279 immunoblotting with anti-Flag or anti-GFP antibodies.

280 In the pull-down assay, the CDSs of *Nbwo*, *NbWo*^{V} and *NbCycB2* were respectively
281 inserted into the pET22b and PGEX-4T-1 vectors to create the fusion proteins
282 (His-Nbwo, His-NbWo^{V} and GST-NbCycB2), and then transformed into the *Escherichia*
283 *coli* BL21 strain. The purified recombinant bait proteins (2 mg His-Nbwo or
284 His-NbWo^{V}) and 2 mg of prey proteins (GST-NbCycB2) were then mixed with 1 ml
285 binding buffer (50 mM Tris-HCl pH 7.5, 0.6% Triton and X-100, 100 mM NaCl,). After
286 incubation at 4 °C for 2 h, 50 µl of glutathione agarose was added to the mixtures
287 followed by the incubation for additional 1 h. The immunoprecipitates were washed
288 five times with binding buffer. The isolated proteins were detected by
289 immunoblotting with anti-His or anti-GST antibodies.

290 **Chromatin immunoprecipitation (ChIP PCR) assay**

291 Four weeks old *NbWo*^{V}*-OE* plants were used for ChIP assay as described in previous
292 study (Gendrel et al., 2005). The NbWo^{V} proteins were precipitated by using HA
293 antibody (Santa Cruz). Primers were designed to amplify 3 fragments (length ~ 120 -
294 210 bp) within the 1.7k bp upstream sequence of the *NbCycB2* transcription start site
295 (Fig. 2a), and 7 fragments within ~ 8.7k bp of genomic DNA sequence of *Nbwo* (Fig.
296 7a). After the immuno-precipitation, the purified DNA was analyzed by real-time PCR
297 with the primers of *NbCycB2* promoter and *Nbwo* genomic DNA sequence fragments
298 (Table S1). Enrichment was calculated from the ratio of immuno-precipitated
299 sequences.

300 **Phenotype observation**

Images of the transgenic plants stem were obtained using Nikon camera. The observation of abaxial leaves and root hair were used an Axioplan 2 microscope (Carl Zeiss AG).

Leaf of transgenic line and wild type seedlings, which used for scanning electron microscope analysis, were fixed with 2% glutaraldehyde (0.1M phosphate buffer, PH 7.4) at 4 □ for 12h. Then, the samples were dehydrated with a series of alcohol (10%, 20%, 30%, 40%, 50%, 60%, 70%, 80%, 90% and 100%) for 20 min each time. Finally, the samples were dried in a critical point drying device (Leica EMCPD030), and coated with gold particles. The samples were observed by using a JSM-6390/LV scanning electron microscope.

Data deposition

The sequences reported in this article have been deposited in the Sol genomic network (Fernandez-Pozo et al., 2015) (https://solgenomics.net/) with the accession numbers as follows: *Nbwo* (Niben101Scf07790g01007.1), *Nbwo*-allele (Niben101Scf00176g11005.1), *NbCycB2* (Niben101Scf10299g00003.1), *NbCycB2*-allele (Niben101Scf10396g00002.1), *NbML1* (Niben101Scf00703g00003.1), *NbML1*-allele (Niben101Scf01158g03010.1).

Results

Expression and cellular analysis of *Nbwo* and *NbCycB2*

We obtained 14 Nbwo and 8 NbCycB2 protein-related sequences from online databases (Fig. S2a, b). The full-length coding sequences of *Nbwo* and *NbCycB2* obtained in the current study contained 2,199 bp and 333 bp, respectively. One allele of each of the *Nbwo* and *NbCycB2* genes were identified via BLAST with 95.82% and 95.20% identity, respectively. The amino acid analysis determined the two-point mutations at 2,084 and 2,092 of N*bWo*^{V} could cause two amino acid replacements in the woolly motif (Ile to Arg, Asp to Tyr, Fig. S1c). Conserved domain analysis revealed that NbCycB2 contained a WD40-like domain in the N-terminal (NbCycB2-WD40, including an EAR like motif) and a RING-like domain in the C-terminal (NbCycB2-RING) (Fig. S2d). However, no conserved domain of B-Type Cyclin protein was found in

331 NbCycB2 protein sequences.

332 The visualization of subcellular localization revealed that NbCycB2, Nbwo and
333 $NbWo^V$ all localized to the nucleus (Fig. S3a). As shown in the self-activation assay,
334 clones of AD-Nbwo and AD-$NbWo^V$ can grow on QDO/X/A medium compared to the
335 positive control, which means they have strong self-activating ability, while the
336 mutations of woolly motif did not affect Nbwo's transactivation ability (Fig. S3b).

337 As shown in Fig. S4a, the spatial expression pattern assays of *NbCycB2* and *Nbwo*
338 indicated they were lowly expressed in roots but at a high level in the trichome
339 containing organs. Further investigation revealed the expression of the *NbCycB2*
340 promoter-driven GFP-GUS transgenic lines was only detected in the trichomes of
341 leaves and stems (Fig. S4b-c). However, GUS of the Nbwo promoter-driven GUS
342 transgenic line was strongly expressed in the basal and venous regions of young
343 leaves (Fig. S4d).

344 ***NbCycB2* negatively regulates trichome initiation**

345 Most of *NbCycB2* overexpression (OE) transgenic lines underwent a dramatic
346 reduction of trichomes on leaves and stems (Fig. S5a, Fig. 1c, 1f). The root length and
347 number of branch root significantly increased in *NbCycB2-OE* lines (Fig. S6). Western
348 blot and qRT-PCR analysis showed the *NbCycB2* transcripts significantly accumulated
349 in *NbCycB2-OE* lines, while the expression levels of *Nbwo* and endogenous *NbCycB2*
350 were significantly reduced (Fig. S5b, c).

351 In contrast, the density of trichomes increased significantly on the leaves and
352 stems of 16 *NbCycB2* knockdown lines (*NbCycB2-RNAi*) (Fig. S5d, Fig. 1b, 1f). The
353 qRT-PCR analysis showed the number of trichomes negatively correlated with the
354 expression level of *NbCycB2* (Fig. S5e), suggesting that *NbCycB2* may play a negative
355 role in trichome initiation.

356

357 ***$NbWo^V$* positively regulates trichome initiation**

358 To confirm the function of *Nbwo*, we also generated 22 *Nbwo* knockdown
359 transgenic plants (*Nbwo*-RNAi). Compared with the wild type, trichome densities
360 were clearly decreased on the leaves and stems of most *Nbwo* knockdown plants

361 (Fig. S7a, e). The efficiency of RNAi mediated knockdown was confirmed by qRT-PCR
362 in two independent lines, in which the expression of *Nbwo* and *NbCycB2* was
363 significantly reduced (Fig. S7b).

364 As in the previous study, dramatic increases in the density and branching of
365 trichomes were found on the leaves and stems of *NbWo*^{V}*-OE* plants (Fig. 1d, 1f, S7d,
366 S7h). Our qRT-PCR assay showed the expression levels of the *NbWo*^{V}, endogenous
367 *Nbwo* and *NbCycB2* genes were all significantly upregulated in transgenic lines (Fig.
368 S7f-g). The dwarfism phenotypes were observed in the T1 plants of *NbWo*^{V}*-OE* (Fig.
369 S8).

370 **Over-expression of *Nbwo* also induces the dwarfism**

371 Twenty transgenic plants with overexpression of *Nbwo* (*Nbwo-OE*) were
372 generated. Interestingly, the density of trichomes was shown to negatively correlate
373 with the expression level of *Nbwo* in the T0 of *Nbwo-OE* plants (Fig. 2a, b).
374 Additionally, the expression levels of *NbCycB2* were significantly reduced in trichome
375 reduced plants (Fig. 2b). However, the decreased trichome phenotypes were not
376 observed in T1 plants, but the higher expression level of exogenous *Nbwo* (for
377 example, *Nbwo-OE #3*) also resulted in dwarfism similar to *NbWo*^{V}*-OE* lines (Fig. 2c).
378 Except for the dwarfism, these two lines, however had a great difference in both
379 trichomes and root hairs. In the *Nbwo-OE #3*, the development of glandular
380 trichomes and the development of root hairs were normal. In *NbWo*^{V}*-OE #1*, the
381 density of glandular trichomes as opposed to root hairs increased significantly (Fig.
382 2d-f).

383 **Nbwo and NbWo^{V} directly targeted the L1-like box of the *NbCycB2* promoter**

384 The expression of *NbCycB2* was significantly upregulated in the *NbWo*^{V}-OE lines,
385 and decreased in the *Nbwo*-RNAi lines (Fig. S7b, f). These results indicated that
386 *NbCycB2* was positively regulated by Nbwo and NbWo^{V}. To test whether Nbwo
387 directly bound to the promoter of *NbCycB2*, *NbWo*^{V}*-OE* (*NbWo*^{V} fused with HA tag)
388 plants were analyzed by ChIP qRT-PCR assay with an HA antibody. Strong enrichment
389 of NbWo^{V} was observed in the P2 region of the *NbCycB2* promoter in *NbWo*^{V}*-OE*
390 plants (Fig. 3a, b).

391 To further determine the specific area of the *NbCycB2* promoter binding to Nbwo,
392 we performed yeast one-hybrid (Y1H) assays. The five truncated fragments of
393 *NbCycB2* promoter were shown in Fig. 3a. The yeast colonies containing
394 *NbCycB2*-proD-pHIS 2 and AD-*Nbwo* constructs were grown on the selection medium
395 with 3-aminotriazole (60 mM) (Fig. 3c).

396 To investigate whether Nbwo and NbWo^{V} directly affect the expression of the D
397 fragment in vivo, we performed dual-Luc assays. The reporters 35S:
398 REN-*NbCycB2*proD: LUC, 35S: REN-*NbCycB2*proB: LUC and the effectors were shown
399 in Fig. 3d. As shown in Figure 3e, each pair of reporter and effector was transiently
400 co-expressed in *N. benthamiana* protoplasts. Compared to the B fragment, when the
401 Nbwo or NbWo^{V} was transiently co-expressed, the D fragment-driven LUC
402 expression accumulated significantly in the protoplasts, indicating that the D
403 fragment of the *NbCycB2* promoter should be a specific site for Nbwo and NbWo^{V}
404 binding.

405 Further analysis of the targeting sequence of *NbCycB2proD* revealed this sequence
406 contained two L1-like boxes (5'-ATTTACTC-3') (Fig. 4a). In the Y1H assay and the in
407 vivo LUC assay, when two L1-like boxes were mutated (*NbCycB2proD-m2*), the
408 interaction with the Nbwo protein is abolished (Fig. 4b, c). Based on these results,
409 we inferred the L1-like boxes may be the binding target of the Nbwo and NbWo^{V}
410 proteins.

411 **NbCycB2 represses the activity of Nbwo rather than NbWo^{V}**

412 Since the *NbCycB2-OE* and *Nbwo-RNAi* transgenic lines shared the non-trichome
413 phenotype, and the expression of *Nbwo* was not enhanced in the *NbCycB2-RNAi*
414 lines (Fig. S5e), we suspect that NbCycB2 could affect Nbwo transactivation ability at
415 protein levels. To confirm this, constructs of overexpression *Nbwo*, *NbWo^{V}* and
416 *NbCycB2* were transiently co-expressed in the leaves of the *NbCycB2*pro: *GFP-GUS*
417 transgenic line using the *Agrobacterium*-mediated method (Fig. 4d). The GUS
418 induced by the transient expression of *Nbwo-OE* was only detected in the area
419 where there was no *NbCycB2-OE* Expression. However, the transient expression of
420 *NbWo^{V}* caused a strong GUS staining which is independent of *NbCycB2-OE*

421 expression. These results were further supported by the LUC assay, in which
422 co-expression with *NbCycB2* could clearly repress the transactivation activity of
423 Nbwo, but did not affect the $NbWo^V$ protein (Fig. 4e). These results suggest that
424 NbCycB2 may act as a negative regulator of Nbwo rather than $NbWo^V$.

425 **NbCycB2 suppresses the transactivation ability of Nbwo via the direct interaction**

426 The interaction between NbCycB2 and Nbwo was reported in a previous study
427 (Yang et al., 2011). To explore which domain was involved in the physical interaction
428 between NbCycB2 and Nbwo, four truncated fragments of Nbwo containing HD, LZ,
429 START and SAD were used (Fig. 5a). Y2H assays suggested that the LZ domain of
430 Nbwo interacted with NbCycB2 (Fig. 5b). The BiFC assay was further used to verify
431 the interaction between the Nbwo LZ domain and NbCycB2 in vivo (Fig. 5c).

432 To further examine if NbCycB2 also interacts with $NbWo^V$, we used yeast
433 two-hybrid (Y2H) assays. Our results indicate that NbCycB2 physically interacts with
434 Nbwo but did not interact with $NbWo^V$, suggesting that the interaction between
435 NbCycB2 and Nbwo can be reduced by mutations in the woolly motif (Fig. 6a).
436 Consistent with the Y2H result, the interaction between NbCycB2 and Nbwo or
437 $NbWo^V$ was further confirmed by the pull-down assay (Fig. 6b) and the bimolecular
438 fluorescence complementation (BiFC) assay (Fig. S10a).

439

440 **Nbwo was restrained by NbCycB2 through forming a homodimer**

441 It is known that the HD-Zip proteins bind to DNA as dimers by the LZ domain (Ariel
442 et al., 2007). To verify whether Nbwo can be dimerized via the LZ domain, we first
443 demonstrated in the Y2H that the LZ domain could bind to the Nbwo protein (Fig.
444 S10b). In addition, BiFC assays were used to confirm the interaction between the LZ
445 domain and Nbwo (or $NbWo^V$) proteins in vivo (Fig. 5c).

446 To test whether the NbCycB2 could bind at the Nbwo homodimer, we conducted
447 the yeast three-hybrid (Y3H) and co-IP assays. As shown in Fig. 6c-d, NbCycB2 could
448 interact with the Nbwo dimers.

449 **Nbwo could bind to its own genomic DNA**

450 The endogenous expression level of *Nbwo* reduced in *NbCycb2-OE* lines (Fig. S5b)

451 and increased in *NbWo^V-OE* plants (Fig. 1d), indicated that Nbwo may be able to
452 regulate self expression. In order to prove this hypothesis, ChIP assay was carried out
453 to check whether Nbwo could bind to its genomic DNA sequence in the leaf of
454 *NbWo^V-OE* transgenic line. Interestingly, enrichment of NbWo^V was found in the T5
455 fragment in *NbWo^V-OE* plants (Fig. 7a, b). This result was further demonstrated by
456 using Y1H assay. Only the clones with AD-Nbwo (or AD-NbWo^V) and Nbwo-G3-pHIS 2
457 constructs could grow on the resistant medium, suggesting that Nbwo or NbWo^V
458 could bind to the G3 fragments (include T5 fragment, Fig. 7a) of its own genomic
459 DNA sequences (Fig. 7c).

460 **Overexpression of *NbCycB2* can reduce the dwarf phenotype of *Nbwo-OE* plants**

461 To determine whether *NbCycB2* can inhibit the transactivation activity of *Nbwo* in
462 vivo, we crossed *NbCycB2-OE #2* T1 plant to *Nbwo-OE #3* T0 plants. As shown in Fig.
463 8 a-b, the dwarf and short-root phenotypes of *Nbwo-OE #3* were indeed reduced by
464 the *NbCycB2-OE #2*. The crossed F1 plants were tested using PCR (Fig. 8 c), and the
465 expression of *NbCycB2* and *Nbwo* was also verified by qRT-PCR. Compared with T1
466 *Nbwo-OE* #3 plants, the balance between *NbCycB2* and *Nbwo* expression was
467 restored in *NbCycB2-OE* #2 and *Nbwo-OE* #3 crossed F1 plants (Fig. 8 d).

468

469 **Discussion**

470 ***NbCycB2* negatively regulates trichome initiation**

471 It is well known that ectopic expression of a constitutive active B-type cyclin
472 promoted the unicellular trichome differentiate to multicellular in *Arabidopsis*
473 (Schnittger et al., 2002, 2005). The *SlCycB2* gene has been reported to be a
474 hypothesis B-type cyclin gene participating in trichome formation in tomato (Yang et
475 al., 2011; Gao et al., 2017). However, the function of *SlCycB2* during trichome
476 development has not been well-studied.

477 In this study, we found that overexpression of *NbCycB2* caused a non-trichome
478 phenotype, whereas inhibition of *NbCycB2* significantly increased the density of
479 trichomes instead of branching on stems and leaves (Fig.1b, S5). Consistent with the
480 qRT-PCR results (Fig. S4a), GUS staining assay indicated *NbCycB2* is specifically

481 expressed in the trichomes of leaves and stems (Fig. S4b-c), and *Nbwo* is expressed
482 in the basal and venous regions of young leaves (Fig. S4d). These results suggested
483 NbCycB2 serves as a negative regulator of trichome initiation. None of B-type cyclin
484 conserve domains were found in the SlCycB2 and NbCycB2 protein sequences (Fig.
485 S2d). Thus, whether SlCycB2 has the function of B type cyclin protein requires
486 further study.
487
488 **NbWo^V and Nbwo directly regulate the expression of *NbCycB2* through binding to**
489 **the L1-like boxes in the promoter**
490 In previous study, *SlCycB2* has been reported to be indirectly regulated by *Wo^V*
491 (Yang et al., 2011; Yang et al., 2015). The expression level of *NbCycB2* was
492 upregulated in overexpression of *NbWo^V* plants and downregulated in *Nbwo-RNAi*
493 lines (Fig. S7), indicating that *NbCycB2* may be the downstream gene of *Nbwo*.
494 Additionally, the D fragments of the *NbCycB2* promoter have been shown to be the
495 binding target of Nbwo and NbWo^V through ChIP, Y1H and LUC assays (Fig. 3).
496 Mutation of the two L1-like box sequences in *NbCycB2*proD inhibited the binding of
497 Nbwo or NbWo^V in vitro and vivo (Fig. 4b). Therefore, we proved that *NbCycB2* was
498 directly regulated by Nbwo or NbWo^V through the binding of L1-like boxes in the
499 *NbCycB2* promoter (Fig. 4a-c). In addition, we also proved that Nbwo and NbWo^V can
500 self-regulate the endogenous expressions by binding to its own genomic DNA
501 sequence by ChIp and YIH assay (Fig. 7).
502 **The increase of trichome density and plant dwarfism was regulated by Nbwo**
503 **through different pathways**
504 The *Wo* homozygous plants have been shown to cause the embryo lethality in
505 seeds (Yang et al., 2011). We also found the overexpression of *Nbwo* or *NbWo^V* genes
506 causes abnormal embryonic development and results in dwarf phenotype in its
507 offspring (Fig. 2c, S6). However, the trichome phenotype of *Nbwo-OE* and *NbWo^V-OE*
508 was completely different (Fig. 2e and 2f), suggesting that Nbwo was involved in both
509 the regulation of the development of trihcome and embryo. The trichomes' density
510 was decreased with the expression of Nbwo in T0 of *Nbwo-OE* lines (Fig.2a and 2e),

511 which suggested that high expression of *Nbwo* in wild type background could repress
512 trichome development. Thus, we suspected the woolly motif represses *Nbwo* activity.
513 However, the trichome density was not increased when the SAD domain deleted
514 *Nbwo* CDS (including woolly motif) was overexpressed in the wild type plants (Fig.
515 S9), which suggesting that woolly motif did not have repressing activity. Therefore,
516 the decreased trichome density in high expression of *wo* gene plants requires further
517 investigation.

518 **NbCycB2 represses the transactivation activity of Nbwo at protein level**

519 The *NbCycB2* gene was proven to be directly regulated by Nbwo in our study.
520 However, the similar non-trichome phenotypes of *NbCycB2-OE* and *Nbwo-RNAi*
521 transgenic lines were found (Fig. S5a, S7a). Additionally, the expression of *Nbwo* was
522 not increased in *NbCycB2-RNAi* plants (Fig. S5e). These results suggested that
523 NbCycB2 might repress the transactivation activity of Nbwo at protein levels. The
524 GUS activity of the *NbCycB2pro*: *GFP-GUS* transgenic line was upregulated by the
525 expression of *Nbwo* and inhibited by the co-expression of *NbCycB2* (Fig. 4d), and the
526 same result was found in the LUC assay (Fig. 4e). Additionally, Hybridization with
527 *NbCycB2-OE* can attenuate the dwarf phenotype of T1 *Nbwo-OE* (Fig. 8a-b). Further
528 studies revealed that the expression of endogenous *NbCycB2* and *Nbwo* were
529 reduced in the *NbCycB2-OE* lines (Fig. S5b). They were shown to be downstream
530 regulatory genes of Nbwo (Figures 3 and 7). These results altogether supported our
531 hypotheses that NbCycB2 may act as a negative regulator of Nbwo at protein levels.

532 In a previous study, SlCycB2 was reported to interact with wo protein (Yang et al.,
533 2011). Further investigation of the interaction between Nbwo and NbCycB2 revealed
534 the dimerized LZ domain of Nbwo binds to NbCycB2 (Fig. 5b, c). Through Y2H, BiFC,
535 Y3H and co-IP assays, we also found that Nbwo could form a homodimer through the
536 LZ domain, and the NbCycB2 protein could bind to LZ domain of Nbwo dimers (Fig.
537 5b-c, 6 c-d, S10b). These results indicated that NbCycB2 may bind to Nbwo protein
538 via its LZ domain to form a complex, which inhibits its transactivation ability.
539 However, further study is required to determine whether *NbCycB2* functions
540 similarly to its homologue gene --AT5G06270.1 which also interacts with the

541 co-repressor TOPLESS (Long et al., 2006; Szemenyei et al., 2008; Pauwels et al., 2010;
542 Wu and Citovsky, 2017a).

543 **The interaction between Nbwo and NbCycB2 was blocked by the mutation in the**
544 **Nbwo woolly motif**

545 In *Arabidopsis thaliana*, the feedback loop regulation mechanisms of the R3 MYB
546 (TRY, CPC and so on) is through competitively binding to GL3/EGL3 to form a
547 non-functional trimeric protein complex (MYB-bHLH-WDR), inhibiting the formation
548 of trichomes (Wang et al., 2008; Wester et al., 2009). Feedback loop regulation has
549 been reported as an effective strategy to maintain normal organism development by
550 many HD-ZIP proteins (Ohgishi et al., 2001; Williams and Fletcher, 2005; Kim et al.,
551 2008; San-Bento et al., 2014). However, the trichome formation was not repressed
552 by the high expression level of *NbCycB2* in the *NbWo*^{V}*-OE* plants (Fig.1d, S7d, f),
553 which suggest that the negative effect of *NbCycB2* could be eliminated by the
554 mutation in *NbWo*^{V}. The LUC assay and GUS activity assay in the leaves of
555 *NbCycB2pro: GFP-GUS* transgenic lines also supported this conclusion (Fig. 4d, e).

556 Further investigation demonstrated the interaction between NbCycB2 and Nbwo
557 could be blocked by the mutation of woolly motif in NbWo^{V} protein in vitro and in
558 vivo (Fig. 6a-b, S10a), indicating that NbWo^{V} abolishes interaction with NbCycB2 to
559 prevent inhibition of NbCycB2. The high expressions of *NbCycB2* and endogenous
560 *Nbwo* in *NbWo*^{V}*-OE* lines also supported this conclusion (Fig. S7f).

561 In summary, through this study, we found NbCycB2 is specifically expressed in the
562 trichomes of *N. benthamiana* and negatively affects trichome formation. Further
563 study revealed the Nbwo and NbWo^{V} were demonstrated to directly regulate
564 *NbCycB2* and *Nbwo* expressions by binding to the L1-like box in the *NbCycB2*
565 promoter and its own genomic DNA sequences. In addition, the NbCycB2 protein
566 may via binding to the LZ domain of Nbwo dimers, which represses the activity of
567 Nbwo and reduces the expression of *Nbwo* downstream genes, eventually leading to
568 the inhibition of trichome initiation. By contrast, the interaction between NbCycB2
569 and Nbwo could be blocked by the mutation in woolly motif (NbWo^{V}), which
570 prevents the repression by NbCycB2, and results in the dramatic increase of

trichome density and branching. In previous studies, since *SlCycB2* is highly expressed in the *Wo* (wo gain-of-function mutant alleles) and Wo^V lines and underexpressed in the *Wo-RNAi* lines, SlCycB2 is believed to promote the development of type I trichomes in tomato (Yang et al., 2011). However, the function and detailed molecular mechanisms of NbCycB2 in regulating trichome development have not been studied. Our findings provide further insights into the regulatory network of *NbCycB2* and *Nbwo* or $NbWo^V$ in multicellular trichomes development of *N. benthamiana* (Fig. S11).

Acknowledgements:

We would like to thank Prof. Xi Huang for kindly providing pBridge and pGreen-0800-II report vectors and thank Dr. Yongjia Zhong, Fujian Agriculture and Forestry university, for kindly providing p2YN and p2YC vectors, and thank Prof. Tao Huang, Prof. Yi Tao and Prof. Hongrui Wang for the help in the implement of experiments. The authors declare no competing financial interests. This study was supported by the State Tobacco Monopoly Administration of China [grant No. 110201401003 (JY-03)], XMU Training Program of Innovation and Enterpreneurship for Undergraduates (2016Y0635) and Guizhou Science and Technology Major Project [Grant No: (2019)3001-2].

Author contributions:

Liang Chen, Hong Cui, Shuang Wu and Minliang Wu conceived and designed the experiments. Minliang Wu, Yuchao Cui, Li Ge, Lipeng Cui, Zhichao Xu, Hongying Zhang, Zhaojun Wang and Dan Zhou performed the experiments and analysed the results. Minliang Wu and Shuang Wu wrote the main manuscript text. Liang Chen supervised the project.

Supplemental Data

Supplemental Fig. S1: The Scanning electron micrographs (SEMs) of trichomes in the leaf of *N. benthamiana.*

601

602 Supplemental Fig. S2: Sequence analysis of *Nbwo*, *NbCycB2* and their similar
603 proteins.

604 Supplemental Fig. S3: The subcellular localization and auto activation test of
605 *NbCycB2*, *Nbwo* and *NbWo*^{V}.

606 Supplemental Fig. S4: The expression pattern of *NbCycB2* and *Nbwo* in *N.*
607 *benthamiana.*

608 Supplemental Fig. S5: Overexpression of *NbCycB2* and RNA interference of *NbCycB2*
609 in *N. benthamiana.*

610 Supplemental Fig. S6: The root phenotypes of wild type, *NbCycB2-RNAi* #7 T1,
611 *NbCycB2-OE* #2 T1, *NbWo*^{V}*-OE* #1 T1, *Nbwo-RNAi #2* T1 seedlings

612 Supplemental Fig. S7: RNA interference of *Nbwo* and overexpression of *NbWo*^{V} in *N.*
613 *benthamiana.*

614 Supplemental Fig. S8: The phenotype of *NbWo*^{V}*-OE* lines.

615 Supplemental Fig. S9: The phenotype of overexpressing *Nbwo-SAD-mutant* in *N.*
616 *benthamiana*.

617 Supplemental Fig. S10: The interaction between Nbwo and NbCycb2, Nbwo and
618 Nbwo LZ domain.

619 Supplemental Fig. S11: A simplified model for regulation between *Nbwo* and
620 *NbCycb2*.

621 Supplemental Table S1: Primers used in this study.

622

623 **Reference:**

624 **Abe, M., Takahashi, T., and Komeda, Y.** (2001). Identification of a cis-regulatory element for
625 L1 layer-specific gene expression, which is targeted by an L1-specific homeodomain
626 protein. The Plant Journal **26,** 487-494.

627 **Ariel, F.D., Manavella, P.A., Dezar, C.A., and Chan, R.L.** (2007). The true story of the HD-Zip
628 family. Trends in plant science **12,** 419-426.

629 **Bombarely, A., Rosli, H.G., Vrebalov, J., Moffett, P., Mueller, L.A., and Martin, G.B.** (2012). A
630 draft genome sequence of Nicotiana benthamiana to enhance molecular
631 plant-microbe biology research. Molecular Plant-Microbe Interactions **25,** 1523-1530.
632 **Chen, S., Songkumarn, P., Liu, J., and Wang, G.L.** (2009). A versatile zero background
633 T-vector system for gene cloning and functional genomics. Plant physiology **150,**
634 1111-1121.
635 **Citovsky, V., Lee, L.-Y., Vyas, S., Glick, E., Chen, M.-H., Vainstein, A., Gafni, Y., Gelvin, S.B.,**
636 **and Tzfira, T.** (2006). Subcellular localization of interacting proteins by bimolecular
637 fluorescence complementation in planta. Journal of molecular biology **362,**
638 1120-1131.
639 **Crooks, G.E., Hon, G., Chandonia, J.M., and Brenner, S.E.** (2004). WebLogo: a sequence
640 logo generator. Genome research **14,** 1188-1190.
641 **Cui, Y., Rao, S., Chang, B., Wang, X., Zhang, K., Hou, X., Zhu, X., Wu, H., Tian, Z., Zhao, Z.,**
642 **Yang, C., and Huang, T.** (2015). AtLa1 protein initiates IRES-dependent translation of
643 WUSCHEL mRNA and regulates the stem cell homeostasis ofArabidopsisin response
644 to environmental hazards. Plant, Cell & Environment **38,** 2098-2114.
645 **Fernandez-Pozo, N., Menda, N., Edwards, J.D., Saha, S., Tecle, I.Y., Strickler, S.R.,**
646 **Bombarely, A., Fisher-York, T., Pujar, A., Foerster, H., Yan, A., and Mueller, L.A.**
647 (2015). The Sol Genomics Network (SGN)—from genotype to phenotype to breeding.
648 Nucleic acids research **43,** D1036-D1041.
649 **Freeman, B.C., and Beattie, G.A.** (2008). An overview of plant defenses against pathogens
650 and herbivores. The Plant Health Instructor

651 http://dx.doi.org/10.1094/PHI-I-2008-0226-01.

652 **Gan, L., Xia, K., Chen, J.G., and Wang, S.** (2011). Functional characterization of
653 TRICHOMELESS2, a new single-repeat R3 MYB transcription factor in the regulation
654 of trichome patterning in Arabidopsis. BMC plant biology **11,** 1-12.

655 **Gao, S., Gao, Y., Xiong, C., Yu, G., Chang, J., Yang, Q., Yang, C., and Ye, Z.** (2017). The
656 tomato B-type cyclin gene, SlCycB2, plays key roles in reproductive organ
657 development, trichome initiation, terpenoids biosynthesis and Prodenia litura defense.
658 Plant Science **262,** 103-114.

659 **Gendrel, A.V., Lippman, Z., Martienssen, R., and Colot, V.** (2005). Profiling histone
660 modification patterns in plants using genomic tiling microarrays. Nature Methods **2,**
661 213-218.

662 **Glas, J.J., Schimmel, B.C., Alba, J.M., Escobar-Bravo, R., Schuurink, R.C., and Kant, M.R.**
663 (2012). Plant glandular trichomes as targets for breeding or engineering of resistance
664 to herbivores. International journal of molecular sciences **13,** 17077-17103.

665 **Goodin, M.M., Zaitlin, D., Naidu, R.A., and Lommel, S.A.** (2008). Nicotiana benthamiana: its
666 history and future as a model for plant–pathogen interactions. Molecular plant-microbe
667 interactions **21,** 1015-1026.

668 **Grebe, M.** (2012). The patterning of epidermal hairs in Arabidopsis--updated. Current opinion
669 in plant biology **15,** 31-37.

670 **Guo, C., Luo, C., Guo, L., Li, M., Guo, X., Zhang, Y., Wang, L., and Chen, L.** (2016).
671 OsSIDP366, a DUF1644 gene, positively regulates responses to drought and salt
672 stresses in rice. Journal of integrative plant biology **58,** 492-502.

673 **Hollósy, F.** (2002). Effects of ultraviolet radiation on plant cells. Micron **33,** 179-197.

674 **Huchelmann, A., Boutry, M., and Hachez, C.** (2017). Plant Glandular Trichomes: Natural Cell
675 Factories of High Biotechnological Interest. Plant physiology **175,** 6-22.

676 **Jefferson, R.A., Kavanagh, T.A., and Bevan, M.W.** (1987). GUS fusions: beta-glucuronidase
677 as a sensitive and versatile gene fusion marker in higher plants. The EMBO journal **6,**
678 3901.

679 **Kang, J.H., Campos, M.L., Zemelis-Durfee, S., Al-Haddad, J.M., Jones, A.D., Telewski, F.W.,**
680 **Brandizzi, F., and Howe, G.A.** (2016). Molecular cloning of the tomato Hairless gene
681 implicates actin dynamics in trichome-mediated defense and mechanical properties of
682 stem tissue. Journal of experimental botany **67,** 5313-5324.

683 **Kim, Y.S., Kim, S.G., Lee, M., Lee, I., Park, H.Y., Seo, P.J., Jung, J.H., Kwon, E.J., Suh, S.W.,**
684 **Paek, K.H., and Park, C.M.** (2008). HD-ZIP III activity is modulated by competitive
685 inhibitors via a feedback loop in Arabidopsis shoot apical meristem development. The
686 Plant cell **20,** 920-933.

687 **Kirik, V., Simon, M., Huelskamp, M., and Schiefelbein, J.** (2004). The ENHANCER OF TRY
688 AND CPC1 gene acts redundantly with TRIPTYCHON and CAPRICE in trichome and
689 root hair cell patterning in Arabidopsis. Developmental Biology **268,** 506-513.

690 **Letunic, I., and Bork, P.** (2018). 20 years of the SMART protein domain annotation resource.
691 Nucleic acids research **46,** D493-D496.

692 **Long, J.A., Ohno, C., Smith, Z.R., and Meyerowitz, E.M.** (2006). TOPLESS Regulates Apical
693 Embryonic Fate in Arabidopsis **312,** 1520-1523.

694 **Mauricio, R., and Rausher, M.D.** (1997). Experimental manipulation of putative selective

695 agents provides evidence for the role of natural enemies in the evolution of plant
696 defense. Evolution, 1435-1444.
697 **Ogawa, E., Yamada, Y., Sezaki, N., Kosaka, S., Kondo, H., Kamata, N., Abe, M., Komeda, Y.,**
698 **and Takahashi, T.** (2015). ATML1 and PDF2 Play a Redundant and Essential Role in
699 Arabidopsis Embryo Development. Plant & cell physiology **56,** 1183-1192.
700 **Ohgishi, M., Oka, A., Morelli, G., Ruberti, I., and Aoyama, T.** (2001). Negative autoregulation
701 of the Arabidopsis homeobox gene ATHB-2. The Plant Journal **25,** 389-398.
702 **Oppenheimer, D.G., Herman, P.L., Shan, S., Esch, J., and Marks, M.D.** (1991). A myb gene
703 required for leaf trichome differentiation in Arabidopsis is expressed in stipules. Cell **67,**
704 483-493.
705 **Pattanaik, S., Patra, B., Singh, S.K., and Yuan, L.** (2014). An overview of the gene regulatory
706 network controlling trichome development in the model plant, Arabidopsis. Frontiers in
707 Plant Science **5,** 259.
708 **Pauwels, L., Barbero, G.F., Geerinck, J., Tilleman, S., Grunewald, W., Perez, A.C., Chico,**
709 **J.M., Bossche, R.V., Sewell, J., Gil, E., Garcia-Casado, G., Witters, E., Inze, D., Long,**
710 **J.A., De Jaeger, G., Solano, R., and Goossens, A.** (2010). NINJA connects the
711 co-repressor TOPLESS to jasmonate signalling. Nature **464,** 788-791.
712 **Payne, C.T., Zhang, F., and Lloyd, A.M.** (2000). GL3 encodes a bHLH protein that regulates
713 trichome development in arabidopsis through interaction with GL1 and TTG1.
714 Genetics **156,** 1349-1362.
715 **Rerie, W.G., Feldmann, K.A., and Marks, M.D.** (1994). The GLABRA2 gene encodes a homeo
716 domain protein required for normal trichome development in Arabidopsis. Genes &

717 development **8,** 1388-1399.

718 **Sallets, A., Beyaert, M., Boutry, M., and Champagne, A.** (2014). Comparative proteomics of
719 short and tall glandular trichomes of Nicotiana tabacum reveals differential metabolic
720 activities. Journal of proteome research **13,** 3386-3396.

721 **San-Bento, R., Farcot, E., Galletti, R., Creff, A., and Ingram, G.** (2014). Epidermal identity is
722 maintained by cell-cell communication via a universally active feedback loop in
723 Arabidopsis thaliana. The Plant Journal **77,** 46-58.

724 **Schmidt, G.W., and Delaney, S.K.** (2010). Stable internal reference genes for normalization of
725 real-time RT-PCR in tobacco (Nicotiana tabacum) during development and abiotic
726 stress. Molecular genetics and genomics : MGG **283,** 233-241.

727 **Schnittger, A., Schöbinger, U., Stierhof, Y.-D., and Hülskamp, M.** (2002). Ectopic B-Type
728 Cyclin Expression Induces Mitotic Cycles in Endoreduplicating Arabidopsis Trichomes.
729 Current Biology **12,** 415-420.

730 **Schnittger, A., Schöbinger, U., Stierhof, Y.-D., and Hülskamp, M.** (2005). Ectopic B-Type
731 Cyclin Expression Induces Mitotic Cycles in Endoreduplicating Arabidopsis Trichomes.
732 Current Biology **15,** 980.

733 **Schnittger, A., Folkers, U., Schwab, B., Jürgens, G., and Hülskamp, M.** (1999). Generation of
734 a spacing pattern: the role of triptychon in trichome patterning in Arabidopsis. The
735 Plant cell **11,** 1105-1116.

736 **Serna, L., and Martin, C.** (2006). Trichomes: different regulatory networks lead to convergent
737 structures. Trends in plant science **11,** 274-280.

738 **Shen, Q., Liu, Z., Song, F., Xie, Q., Hanley-Bowdoin, L., and Zhou, X.** (2011). Tomato

739 SlSnRK1 protein interacts with and phosphorylates βC1, a pathogenesis protein
740 encoded by a geminivirus β-satellite. Plant physiology **157,** 1394-1406.
741 **Szemenyei, H., Hannon, M., and Long, J.A.** (2008). TOPLESS Mediates Auxin-Dependent
742 Transcriptional Repression During Arabidopsis Embryogenesis **319,**
743 1384-1386.
744 **Valkama, E., SALMINEN, J.P., Koricheva, J., and Pihlaja, K.** (2003). Comparative analysis of
745 leaf trichome structure and composition of epicuticular flavonoids in Finnish birch
746 species. Annals of Botany **91,** 643-655.
747 **Wada, T., Tachibana, T., Shimura, Y., and Okada, K.** (1997). Epidermal cell differentiation in
748 Arabidopsis determined by a Myb homolog, CPC. Science **277,** 1113-1116.
749 **Walker, A.R., Davison, P.A., Bolognesi-Winfield, A.C., James, C.M., Srinivasan, N., Blundell,**
750 **T.L., Esch, J.J., Marks, M.D., and Gray, J.C.** (1999). The TRANSPARENT TESTA
751 GLABRA1 locus, which regulates trichome differentiation and anthocyanin
752 biosynthesis in Arabidopsis, encodes a WD40 repeat protein. The Plant cell **11,**
753 1337-1349.
754 **Wang, S., Hubbard, L., Chang, Y., Guo, J., Schiefelbein, J., and Chen, J.G.** (2008).
755 Comprehensive analysis of single-repeat R3 MYB proteins in epidermal cell patterning
756 and their transcriptional regulation in Arabidopsis. BMC plant biology **8,** 1-13.
757 **Wester, K., Digiuni, S., Geier, F., Timmer, J., Fleck, C., and Hülskamp, M.** (2009). Functional
758 diversity of R3 single-repeat genes in trichome development. Development **136,**
759 1487-1496.
760 **Williams, L., and Fletcher, J.C.** (2005). Stem cell regulation in the Arabidopsis shoot apical

761 meristem. Current opinion in plant biology **8,** 582-586.

762 **Wu, R., and Citovsky, V.** (2017a). Adaptor proteins GIR1 and GIR2. II. Interaction with the
763 co-repressor TOPLESS and promotion of histone deacetylation of target chromatin.
764 Biochemical and biophysical research communications **488,** 609-613.

765 **Wu, R., and Citovsky, V.** (2017b). Adaptor proteins GIR1 and GIR2. I. Interaction with the
766 repressor GLABRA2 and regulation of root hair development. Biochemical and
767 biophysical research communications **488,** 547-553.

768 **Yan, T., Chen, M., Shen, Q., Li, L., Fu, X., Pan, Q., Tang, Y., Shi, P., Lv, Z., Jiang, W., Ma,**
769 **Y.N., Hao, X., Sun, X., and Tang, K.** (2016). HOMEODOMAIN PROTEIN 1 is required
770 for jasmonate-mediated glandular trichome initiation in Artemisia annua. New
771 Phytologist **213,** 1145-1155.

772 **Yang, C., Gao, Y., Gao, S., Yu, G., Xiong, C., Chang, J., Li, H., and Ye, Z.** (2015).
773 Transcriptome profile analysis of cell proliferation molecular processes during
774 multicellular trichome formation induced by tomato Wo (v) gene in tobacco. BMC
775 genomics **16,** 868.

776 **Yang, C., Li, H., Zhang, J., Luo, Z., Gong, P., Zhang, C., Li, J., Wang, T., Zhang, Y., and Lu,**
777 **Y.E.** (2011). A regulatory gene induces trichome formation and embryo lethality in
778 tomato. Proceedings of the National Academy of Sciences of the United States of
779 America **108,** 11836-11841.

780 **Yoo, S.D., Cho, Y.H., and Sheen, J.** (2007). Arabidopsis mesophyll protoplasts: a versatile cell
781 system for transient gene expression analysis. Nature protocols **2,** 1565-1572.

782

783

784 **Figure legends**

785 Fig. 1: The trichome phenotypes of *NbCycB2*, *Nbwo* and *NbWo*^{V} transgenic seedlings
786 (a), (b), (c), (d), (e), are the trichomes SEMs of wild type, *NbCycB2-RNAi* #7 T1,
787 *NbCycB2-OE* #2 T1, *NbWo*^{V}*-OE* #1 T1, *Nbwo-RNAi #2* T1 10d-old-seedlings
788 respectively. The white bar is 500 µm. (f) The trichome density of the wild type,
789 *NbCycB2-RNAi* #7 T1, *NbCycB2-OE* #2 T1, *NbWo*^{V}*-OE* #1 T1, *Nbwo-RNAi #2* T1
790 10d-old-seedlings leaves were shown. "*" indicates a difference at P<0.05 by
791 Student's t test compared to WT. "**" represent significant difference against WT at
792 P < 0.01. Error bars represent SD (n = 3).

793

794 Fig. 2: Over expression of *Nbwo* also induce the dwarf phenotype in *N. benthamiana*
795 (a) Over expression of *Nbwo* was drivered by P35S promoter. The trichomes density
796 reduced in the stems and leaves of transgenic lines. (b) The relative expression level
797 of *Nbwo* and*NbCycB2* in the transgenic lines measured by qRT-PCR. Error bars
798 represent SD (n = 3). (c) The root lengths were measured in the Wild type,
799 *NbCycB2-OE* #1 T1, *Nbwo-OE* #3 T1, *Nbwo-RNAi #2* T1 two weeks-old-seedlings. The
800 white bar is 1 cm. (d) The root hairs of *Nbwo-OE* #3 T1 and *NbWo*^{V}*-OE* #1 T1 two
801 weeks-old-seedlings were detected by microscope. The red bar is 1 mm. (e), (f) are
802 the SEMs of the *Nbwo-OE* #3 T1 and *NbWo*^{V}*-OE* #1 T1 10d-old-seedlings respectively.
803 The white bar is 500 µm.

804

805 Fig. 3: Nbwo and NbWo^{V} protein can bind *NbCycB2* promoter in vitro and vivo
806 (a) The fragments of *NbCycB2* promoter were used to CiHP (P1, P2 and P3) and yeast
807 one-hybrid assays (A, B, C, D and E). The numbers indicate positions of the *NbCycB2*
808 promoter truncations. (b) Graphs show the ratio of bound promoter fragments
809 (P1-P3) versus total input detected by qRT-PCR after immuno-precipitation in
810 HA-NbWo^{V} by HA antibodies. Data shown are mean ± SE (n = 3). (c) One-hybrid (Y1H)
811 assays were used to determine the interaction of *NbCycB2* promoter fragments (A, B,
812 C, D, E) bait constructs and AD-*Nbwo* or empty pGADT7 constructs in Y187 yeast
813 strains. (d) The schematic diagram of the effectors and reporters constructs were

814 used in the LUC assay. (e) The relative reporter activities were measured in *N.*
815 *benthamiana* protoplasts after transiently transformed the effector and reporter
816 constructs. The relative LUC activities normalized to the REN activity are shown
817 (LUC/REN). The difference between combinations were detected by Student's t test.
818 "**" present that the LUC activity is significantly different (P< 0.01). Error bars
819 represent SD (n = 3).
820
821 Fig. 4: NbCycB2 can suppress the function of Nbwo, but has no effect on $NbWo^V$
822 (a) The DNA sequences of wild type *NbCycB2* promoter (ProD) and mutant fragments
823 were shown. L1-like boxes were indicated by using gray arrow. The mutated bases in
824 the m1 and m2 sequences are shown by a dividing line. (b) One-hybrid (Y1H) assays
825 were used to detected the interaction between mutant D fragments of *NbCycB2*
826 promoter bait constructs and AD-*Nbwo* or AD-$NbWo^V$ in Y187 yeast strains, the
827 empty pGADT7 construct as the control. (c) Relative reporter activity was measured
828 in *N. benthamiana* protoplasts after transiently co-transformed the effector and
829 reporter constructs. The relative LUC activities normalized to the REN activity are
830 shown (LUC/REN). "**" present that the LUC activity has significant difference
831 between the D and m2 fragments reporter when their co-transformed with *Nbwo* or
832 $NbWo^V$ effector respectively (P< 0.01, Student's t test). Error bars represent SD (n =
833 3). (d) The GUS staining of the *proNbCycB2: GFP-GUS* transgenic line leaves, when
834 co-expressing *P35S: Nbwo* and *P35S: NbCycB2*, *P35S:* $NbWo^V$ and *P35S: NbCycB2*. The
835 area of red circle was injected with *P35S: Nbwo* GV3101 strain; the area of Green
836 circle was injected with *P35S:* $NbWo^V$ GV3101 strain; the area of blue circles were
837 injected with *P35S: NbCycB2* GV3101 strain. (e) The LUC activity of co-transforming
838 the effector and reporter constructs were measured. "**" present that the LUC
839 activity is significantly different between *Nbwo* and $NbWo^V$ effector when they
840 co-transformed with *NbCycB2* effector respectively (P< 0.01, Student's t test). Error
841 bars represent SD (n = 3).
842
843 Fig. 5: NbCycB2 protein interact with LZ domain of the Nbwo protein in vitro and vivo

844 (a) Schematic diagrams of Nbwo protein domain constructs. The numbers indicate
845 positions of the first and the last amino acid of the Nbwo truncations. (b) Interaction
846 between NbCycB2 and domains of Nbwo protein were determined by YH2 system. (c)
847 The interaction between Nbwo and NbCycB2 or itself were demonstrated by BiFC
848 assay. Each indicated pair of constructs were co-infiltrated into leaves of *N.*
849 *benthamiana* (Bar, 50 µm).
850
851 Fig. 6: Mutation of woolly motif reduce the interaction between Nbwo and NbCycB2
852 (a) Interaction between NbCycB2 and Nbwo or $NbWo^{V}$ proteins were determined by
853 YH2 system. Blue clones grown on the QDO/X/A medium indicates positive
854 protein-protein interactions. (b) The pull down assay between Nbwo or $NbWo^{V}$ with
855 NbCycB2 proteins. Only recombinant HIS-Nbwo protein can co-precipitate with
856 GST-NbCycB2 protein. (c) The competitive binding between NbCycB2 and LZ domain,
857 LZ domain and Nbwo were determined by Yeast three-hybrid assays. (d) The co-IP
858 assay between NbCycB2 and Nbwo dimers. The total protein immunoprecipitation
859 was performed by using anti-HA beads.
860
861 Fig. 7: Nbwo and $NbWo^{V}$ can bind at itself genomic DNA sequences
862 (a) The fragments of *Nbwo* genomic sequences were used to CHiP (T1, T2, T3, T4, T5,
863 T6 and T7) and yeast one-hybrid assays (G1, G2, G3 and G4). The bar present 1 kb
864 DNA sequences. (b) Graphs show the ratio of bound genomic fragments (T1-T7)
865 versus total input detected by real-time PCR after immuno-precipitation in
866 *$NbWo^{V}$-OE* lines by HA antibodies. Data shown are mean ± SE (n = 3). (c) One-hybrid
867 (Y1H) assays were used to determine the interaction of *Nbwo* genomic sequence
868 fragments (G1, G2, G3, G4) bait constructs and AD-Nbwo, AD-$NbWo^{V}$ or empty
869 pGADT7 constructs in Y187 yeast strains. The clones grown on the SD/-Leu/-His/-Trp
870 (-L-W-H) with 60 mM 3-AT medium indicates the interaction between DNA fragment
871 and Nbwo or $NbWo^{V}$ proteins.
872
873 Fig. 8: Hybridization between *Nbwo-OE* and *NbCycB2-OE* plants

874 (a), (b) The phenotype of *NbCycB2-OE* #2 and *Nbwo-OE* #3 hybridization F1 two
875 weeks old (a) and mature (b) plants were shown. "I"present wild type *N.*
876 *benthamiana*, "II"present *NbCycB2-OE/WT* hybrid T1 plants, "III"present *NbCycB2-OE*
877 *#2* and *Nbwo-OE #3* hybridization F1 plants, "IV"present *Nbwo-OE #3/WT* hybrid T1
878 plants. (c) F1 plants were tested by using PCR. Wild type as a negative control,
879 *Nbwo-OE* #3 and *NbCycB2-OE* #2 as positive controls. No DNA band was detected in
880 the wild type *N. benthamiana*. A ~330 bp DNA band was detected in *NbCycB2-OE* #2
881 lines. A ~2199 bp DNA band was detected in *Nbwo-OE #3* lines. In contrary, two
882 bands were detected in *NbCycB2-OE #2* and *Nbwo-OE #3* hybridization F1 plants. (d)
883 The relative expression levels of *Nbwo* and *NbCycb2* were measured by qRT-PCR in
884 F1 plants. Data are given as means SD (n = 3).
885

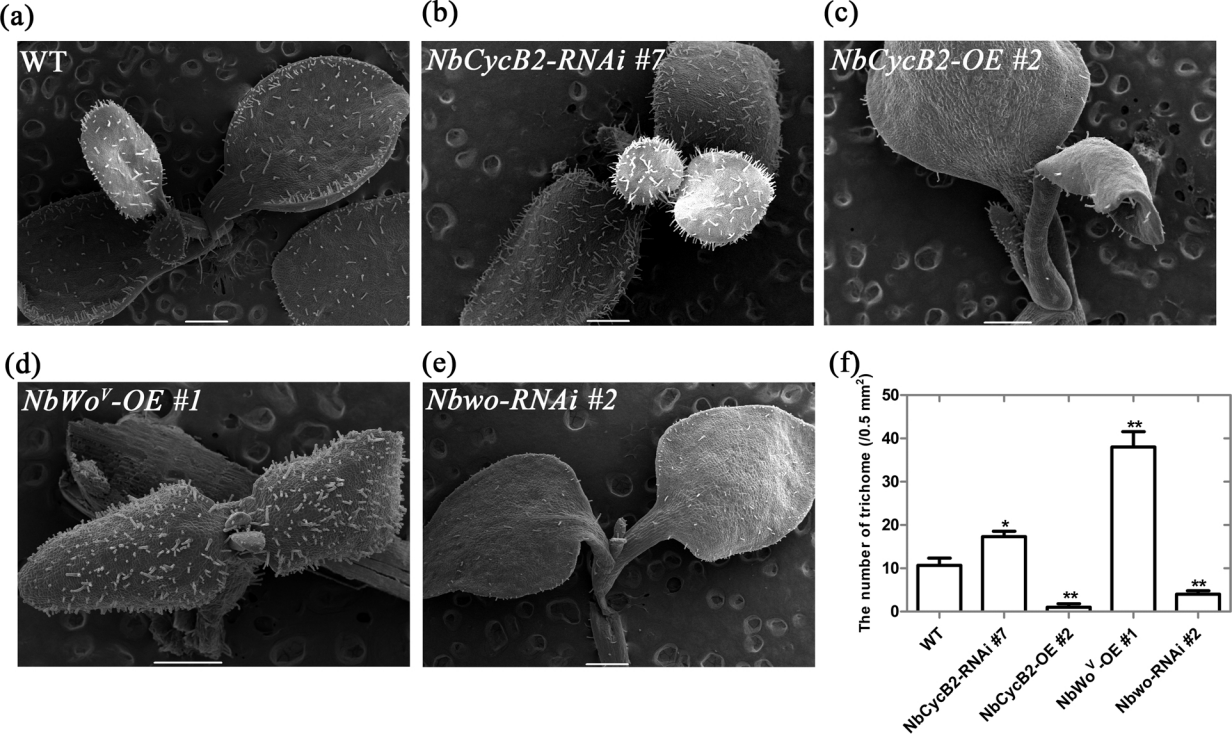
(a)
WT
(b)
NbCycB2-RNAi #7
(c)
NbCycB2-OE #2
(d)
NbWo^V-OE #1
(e)
Nbwo-RNAi #2
(f)
The number of trichome (/0.5 mm²)
50
40
30
20
10
0
*
**
**
**
WT
NbCycB2-RNAi #7
NbCycB2-OE #2
NbWo^V-OE #1
Nbwo-RNAi #2

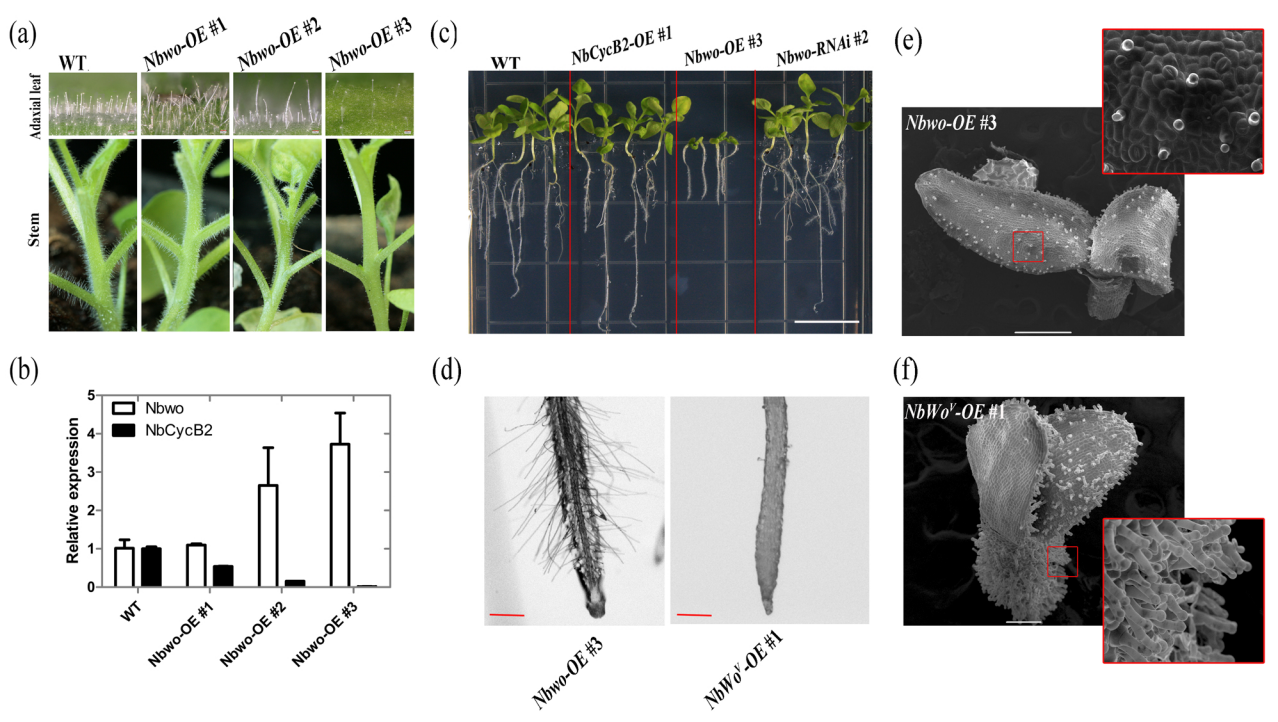
(a)
WT
Nbwo-OE #1
Nbwo-OE #2
Nbwo-OE #3
Adaxial leaf
Stem
(b)
Nbwo
NbCycB2
Relative expression
0
1
2
3
4
5
WT
Nbwo-OE #1
Nbwo-OE #2
Nbwo-OE #3
(c)
WT
NbCycB2-OE #1
Nbwo-OE #3
Nbwo-RNAi #2
(d)
Nbwo-OE #3
NbWo^V-OE #1
(e)
Nbwo-OE #3
(f)
NbWo^V-OE #1

(a)

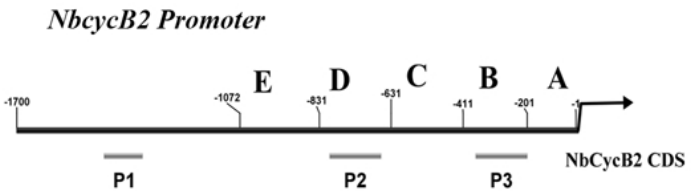
NbcycB2 Promoter
E
D
C
B
A
-1700
-1072
-831
-631
-411
-201
-1
P1
P2
P3
NbCycB2 CDS

(b)

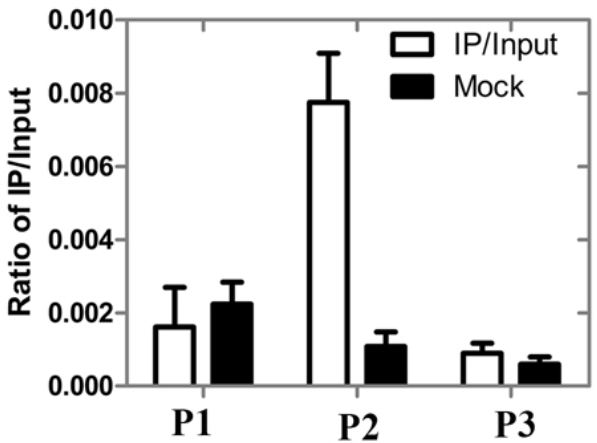
0.010
0.008
0.006
0.004
0.002
0.000
Ratio of IP/Input
IP/Input
Mock
P1
P2
P3

(c)

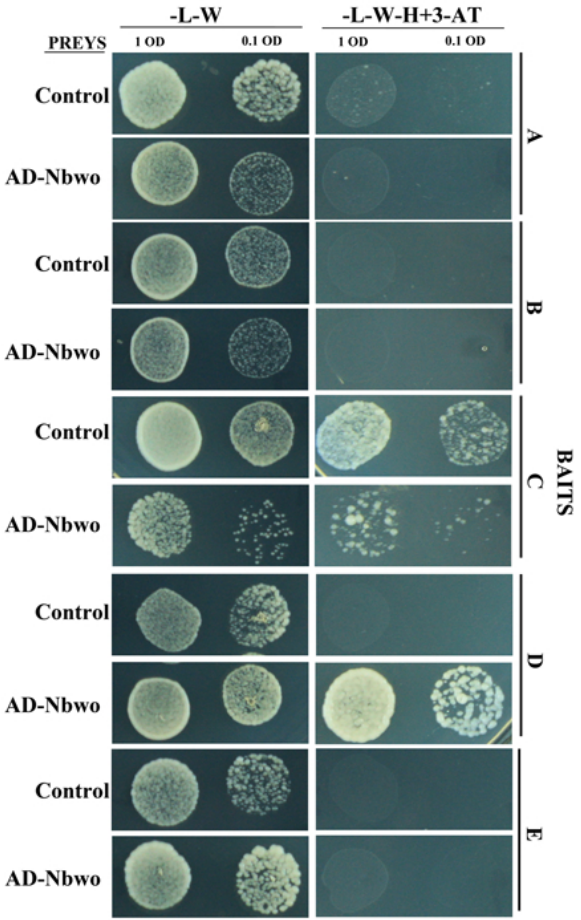
-L-W
-L-W-H+3-AT
PREYS
1 OD
0.1 OD
1 OD
0.1 OD
Control
AD-Nbwo
Control
AD-Nbwo
Control
AD-Nbwo
Control
AD-Nbwo
Control
AD-Nbwo
A
B
C
D
E
BAITS

(d)

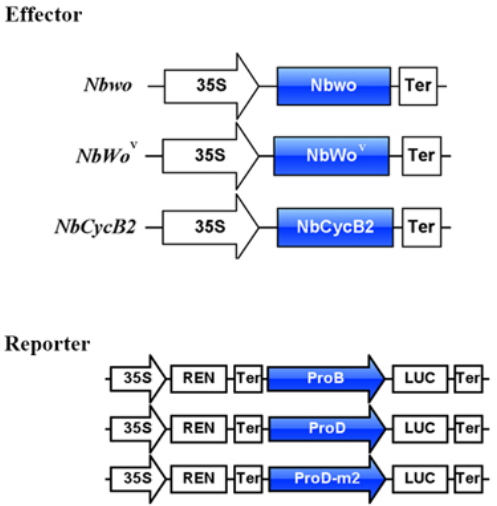
Effector
Nbwo
35S
Nbwo
Ter
NbWo^V
35S
NbWo^V
Ter
NbCycB2
35S
NbCycB2
Ter
Reporter
35S
REN
Ter
ProB
LUC
Ter
35S
REN
Ter
ProD
LUC
Ter
35S
REN
Ter
ProD-m2
LUC
Ter

(e)

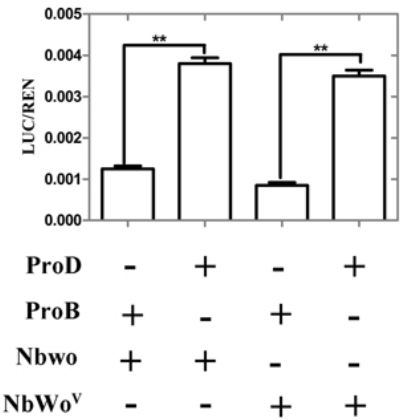
0.005
0.004
0.003
0.002
0.001
0.000
LUC/REN
**
**
ProD - + - +
ProB + - + -
Nbwo + + - -
NbWo^V - - + +

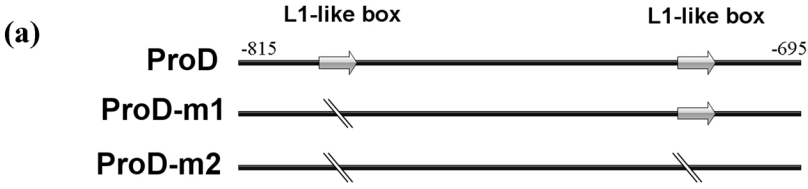
(a)
L1-like box
L1-like box
ProD
-815
-695
ProD-m1
ProD-m2

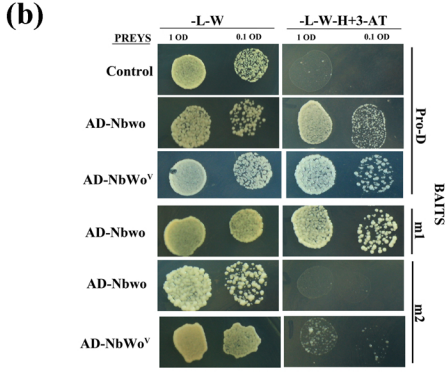
(b)
-L-W
-L-W-H+3-AT
PREYS
1 OD
0.1 OD
1 OD
0.1 OD
Control
AD-Nbwo
AD-NbWo^V
AD-Nbwo
AD-Nbwo
AD-NbWo^V
Pro-D
m1
m2
BAITS

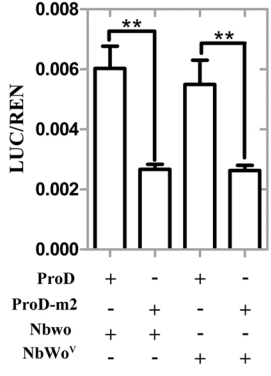
(c)
LUC/REN
0.008
0.006
0.004
0.002
0.000
**
**
ProD + - + -
ProD-m2 - + - +
Nbwo + + - -
NbWo^V - - + +

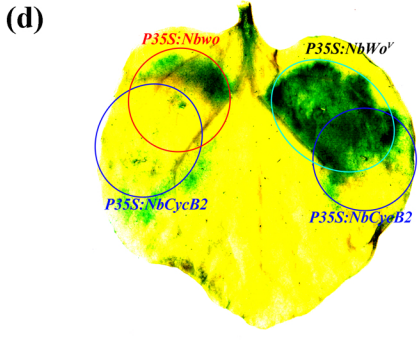
(d)
P35S:Nbwo
P35S:NbWo^V
P35S:NbCycB2
P35S:NbCycB2

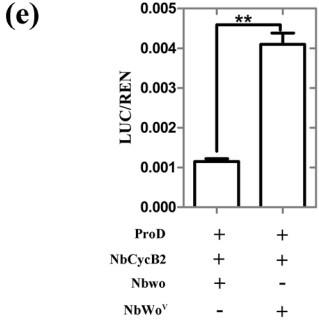
(e)
LUC/REN
0.005
0.004
0.003
0.002
0.001
0.000
**
ProD + +
NbCycB2 + +
Nbwo + -
NbWo^V - +

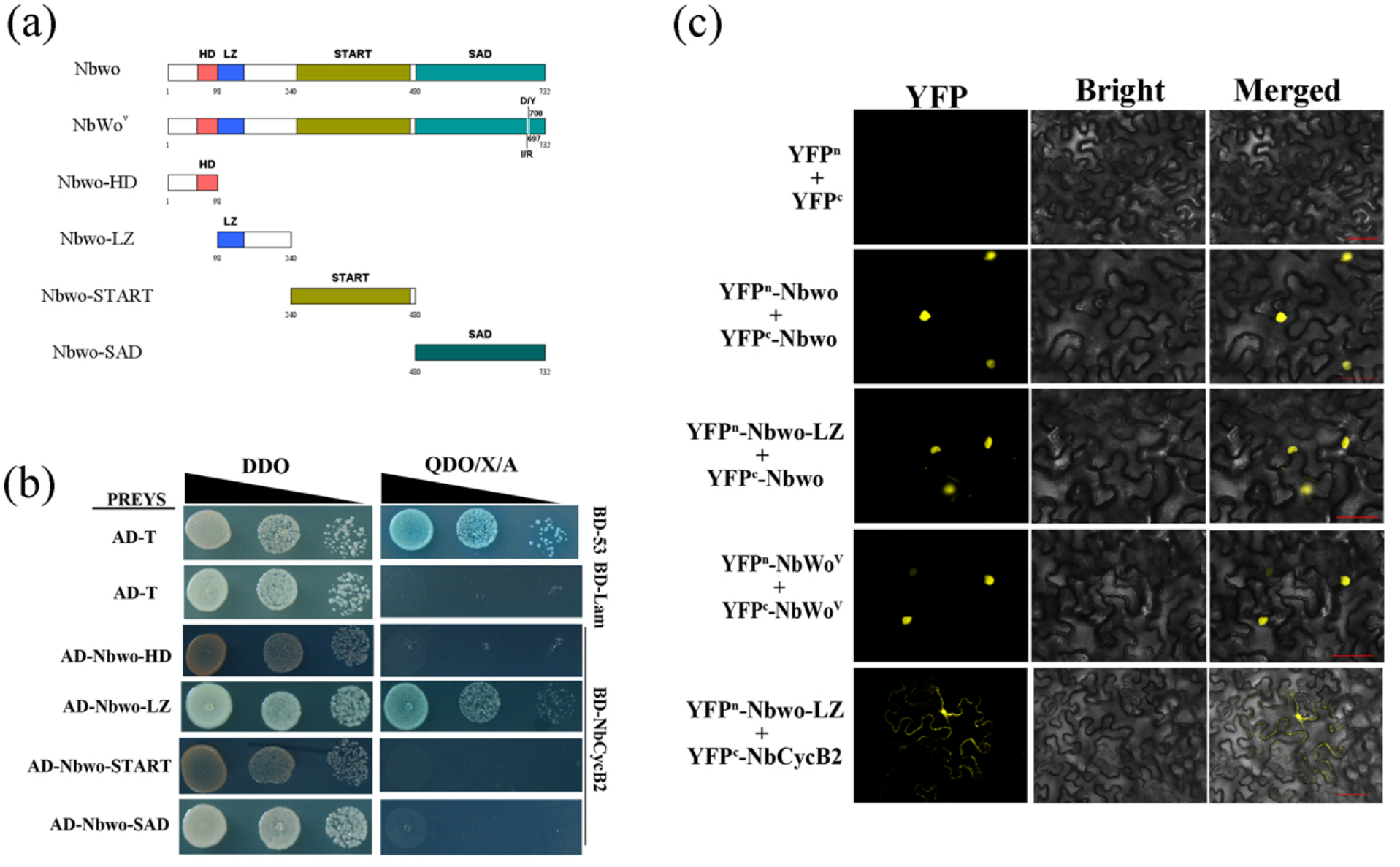
(a)
Nbwo
HD
LZ
START
SAD
1
98
240
480
732
NbWo^{v}
D/Y
700
697
I/R
Nbwo-HD
Nbwo-LZ
Nbwo-START
Nbwo-SAD
(b)
DDO
QDO/X/A
PREYS
AD-T
AD-T
AD-Nbwo-HD
AD-Nbwo-LZ
AD-Nbwo-START
AD-Nbwo-SAD
BD-53
BD-Lam
BD-NbCycB2
(c)
YFP
Bright
Merged
YFP^{n} + YFP^{c}
YFP^{n}-Nbwo + YFP^{c}-Nbwo
YFP^{n}-Nbwo-LZ + YFP^{c}-Nbwo
YFP^{n}-NbWo^{V} + YFP^{c}-NbWo^{V}
YFP^{n}-Nbwo-LZ + YFP^{c}-NbCycB2

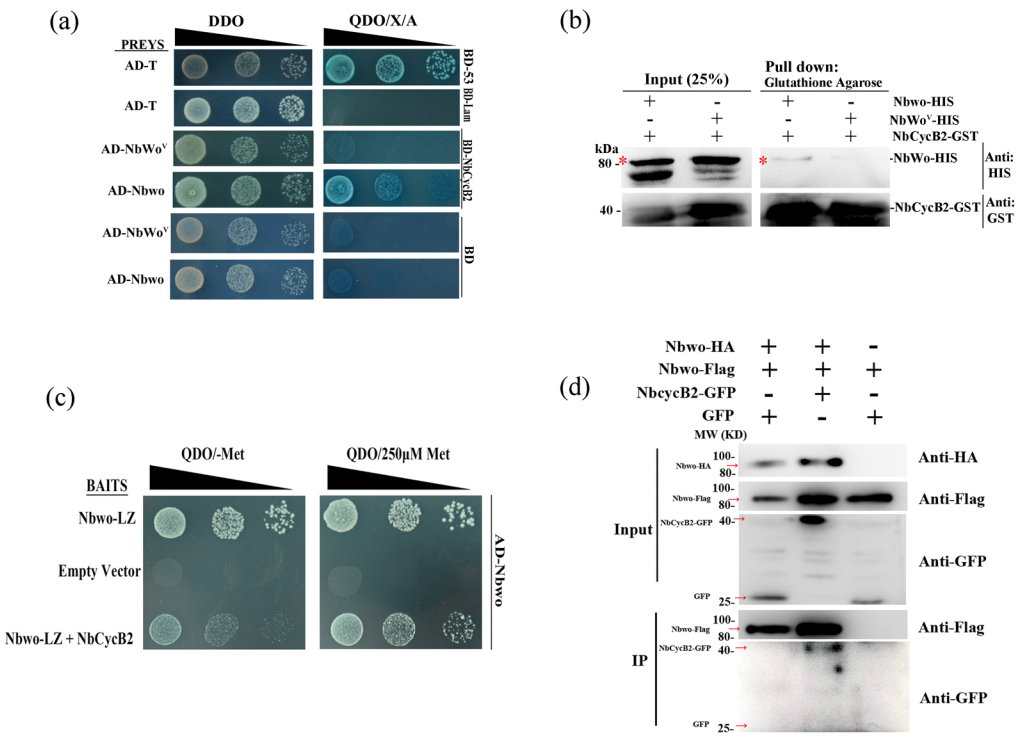
(a)
DDO
QDO/X/A
PREYS
AD-T
AD-T
AD-NbWo^{V}
AD-Nbwo
AD-NbWo^{V}
AD-Nbwo
BD-53
BD-Lam
BD-NbCycB2
BD
(b)
Input (25%)
Pull down:
Glutathione Agarose
Nbwo-HIS
NbWo^{V}-HIS
NbCycB2-GST
kDa
80 -
40 -
-NbWo-HIS
-NbCycB2-GST
Anti: HIS
Anti: GST
(c)
QDO/-Met
QDO/250μM Met
BAITS
Nbwo-LZ
Empty Vector
Nbwo-LZ + NbCycB2
AD-Nbwo
(d)
Nbwo-HA
Nbwo-Flag
NbcycB2-GFP
GFP
MW (KD)
Input
IP
Nbwo-HA
Nbwo-Flag
NbCycB2-GFP
GFP
100-
80-
40-
25-
Anti-HA
Anti-Flag
Anti-GFP
Anti-Flag
Anti-GFP

(a)

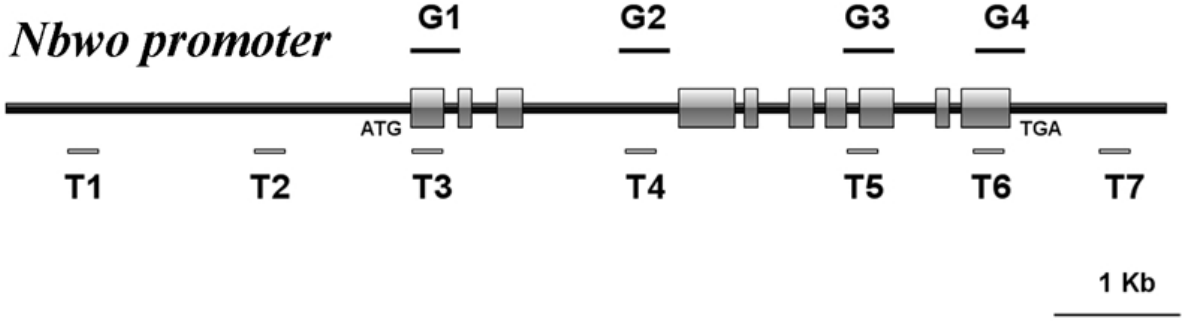
Nbwo promoter
G1
G2
G3
G4
ATG
TGA
T1
T2
T3
T4
T5
T6
T7
1 Kb

(b)

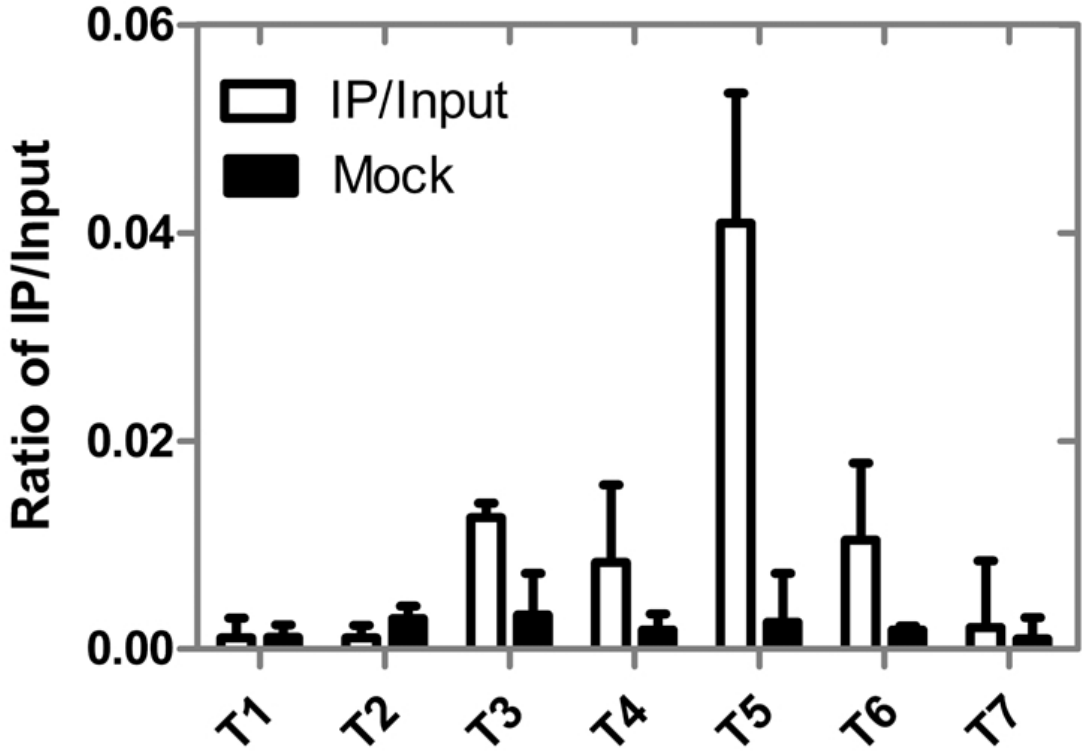
0.06
0.04
0.02
0.00
Ratio of IP/Input
IP/Input
Mock
T1
T2
T3
T4
T5
T6
T7

(c)

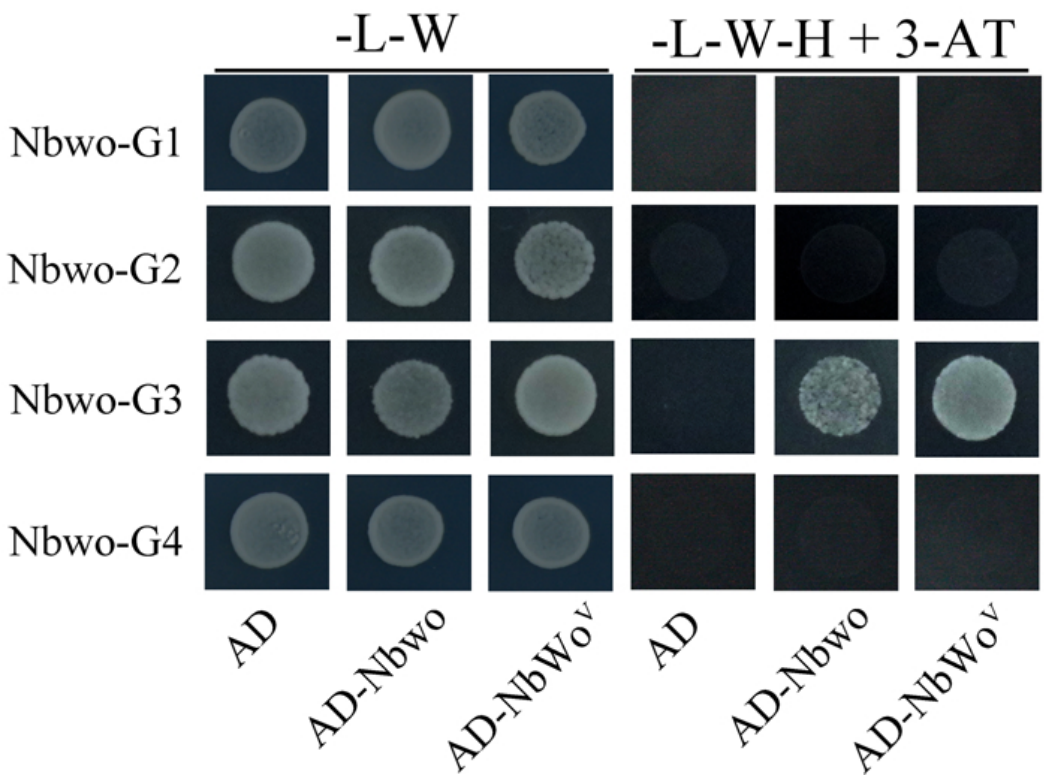
-L-W
-L-W-H + 3-AT
Nbwo-G1
Nbwo-G2
Nbwo-G3
Nbwo-G4
AD
AD-Nbwo
AD-NbWo^{V}
AD
AD-Nbwo
AD-NbWo^{V}

(a)

I: *WT*

II: *NbcycB2-OE #2 / WT*

III: *Nbwo-OE #3 / NbcycB2-OE #2*

IV: *Nbwo-OE #3 /WT*

(b)

(c)

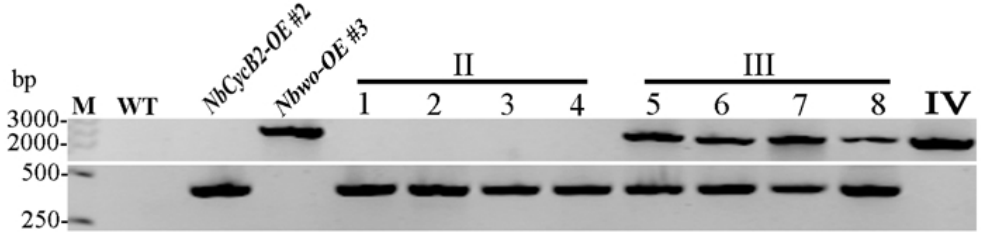
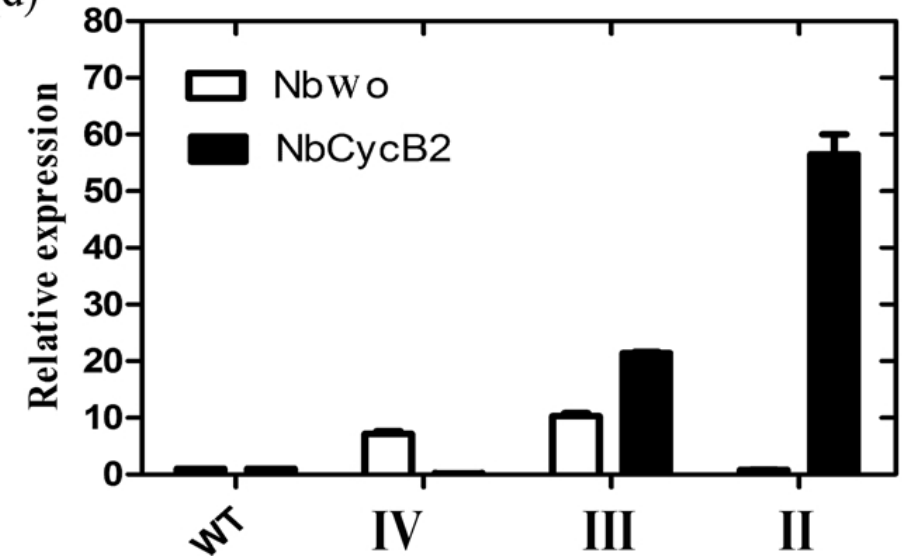
(d)